

# Esters of Cinnamic Acid as Green Plasticizers for Polylactide Formulations with Improved Ductility

Alejandro Barandiaran, Jaume Gomez-Caturla, Juan Ivorra-Martinez,\* Diego Lascano, Miguel Angel Selles, Virginia Moreno, and Octavio Fenollar

This study demonstrates the potential of different cinnamate esters, namely methyl trans-cinnamate (MC), isobutyl cinnamate (IBC), allyl cinnamate (AC), and ethyl cinnamate (EC), as environmentally friendly plasticizers for polylactide (PLA). Plasticized PLA formulations with a constant nominal wt% of 20 of each plasticizer are compounded in a twin-screw co-rotating extruder and subsequently processed by injection molding. The results show exceptional plasticization efficiency of AC with an increase in elongation at break from 3.9% (neat PLA), up to 339.4% and a remarkable increase in impact strength, thus showing great potential to overcome the main drawback related to PLA intrinsic brittleness. The incorporation of cinnamates in a PLA matrix leads to a decrease in  $T_g$  from 61.7 °C down to 36.1 °C for the plasticized PLA formulation containing 20 wt% AC. Thermogravimetry analysis reveals that a slight plasticizer loss occurs during processing, as it happens with other monomeric plasticizers, but this phenomenon does not limit their plasticization efficiency. Therefore, the results obtained in this study confirm the suitability of a new family of organic compounds derived from the esterification of cinnamic acid as green plasticizers for PLA with improved toughness, with comparable, or even superior, ductile properties of typical plasticizers for PLA.

Among these polymers, it is possible to find petroleum-based polyesters such as polybutylene succinate (PBS), polyglycolide (PGA), polycaprolactone (PCL), and polybutylene succinate-co-adipate (PBSA). In fact, currently, some of these polyesters can also be fully or partially synthesized from different biobased building blocks.<sup>[1–4]</sup> Nevertheless, biobased polyesters, such as polylactide (PLA) and polyhydroxyalkanoates (PHAs), have received much attention due to their environmental advantages and represent a sound alternative to petroleum-derived polymers.<sup>[5–7]</sup>

PLA is an aliphatic polyester that is usually obtained by ring-opening polymerization (ROP) of lactide, which is obtained by fermentation of starch-rich plant sources such as rice, corn, cassava (tapioca), and sugarcane, among others.<sup>[8–10]</sup> PLA offers rather good balanced properties (mechanical, thermal, biodegradation, transparency, barrier, and so on) and processability.<sup>[11]</sup> Nevertheless, one of its main drawbacks is related to its intrinsic brittleness, due to poor ductile behavior, which hinders its


massive use, mainly in the packaging industry. Hence, much research on PLA has focused on improving toughness.<sup>[12–16]</sup> To overcome this, physical blending with flexible polymers and plasticization have been proposed.<sup>[17,18]</sup> It has been widely reported in the literature the remarkable improvement in ductile and impact strength properties of PLA by binary and ternary blends with flexible polymers such as PBS,<sup>[19–21]</sup> PCL,<sup>[22]</sup> PBSA,<sup>[23]</sup> polybutylene adipate-co-terephthalate (PBAT),<sup>[24–26]</sup> and thermoplastic starch,<sup>[27]</sup> among others, with or without using compatibilizers.<sup>[28,29]</sup>

A plasticizer must fulfill some features for good efficiencies, such as low molecular weight, high boiling point, low viscosity, non-volatile character, low migration, and non-toxic, among others.<sup>[30,31]</sup> Generally, a plasticizer provides improved processability and ductility due to a decrease in the glass transition temperature ( $T_g$ ).<sup>[32,33]</sup> It has been also reported a decrease in the melt peak temperature in plasticized semicrystalline polymers.<sup>[34]</sup> A wide range of compounds has been proposed as plasticizers for PLA and its blends including citrates,<sup>[31,35]</sup> tartrates,<sup>[36]</sup> adipates,<sup>[37]</sup> sebacates,<sup>[38]</sup> azelates,<sup>[39]</sup> short-chain triglycerides,<sup>[40]</sup> chemically-modified vegetable oils and fatty acids,<sup>[41–44]</sup> oligomers of lactic acid (OLAs),<sup>[45]</sup> and polyethylene

## 1. Introduction

In the last decade, aliphatic polyesters have attracted much attention due to the increasing concern about the environment. Aliphatic polyesters can undergo biodegradation under compost conditions due to the hydrolysis of ester groups, which represents a clear advantage from an environmental point of view.

A. Barandiaran, J. Gomez-Caturla, J. Ivorra-Martinez, D. Lascano, M. A. Selles, V. Moreno, O. Fenollar  
 Institute of Materials Technology (ITM)  
 Technical University of Valencia (UPV)  
 Alcoy, Alicante 03801, Spain  
 E-mail: juainvar@doctor.upv.es

 The ORCID identification number(s) for the author(s) of this article can be found under <https://doi.org/10.1002/mame.202300022>

© 2023 The Authors. Macromolecular Materials and Engineering published by Wiley-VCH GmbH. This is an open access article under the terms of the Creative Commons Attribution License, which permits use, distribution and reproduction in any medium, provided the original work is properly cited.

DOI: 10.1002/mame.202300022

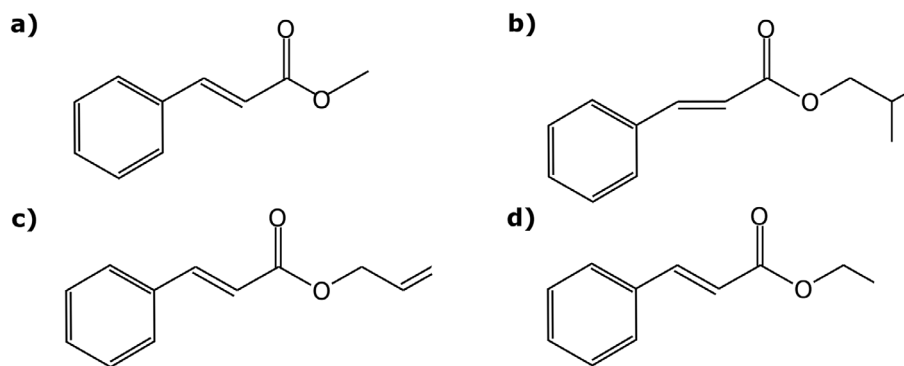


**Figure 1.** Schematic representation of the chemical structure of a) methyl trans-cinnamate (MC), b) isobutyl cinnamate (IBC), c) allyl cinnamate (AC), and d) ethyl cinnamate (EC).

**Table 1.** Physicochemical and thermal properties of methyl trans-cinnamate (MC), isobutyl cinnamate (IBC), allyl cinnamate (AC), and ethyl cinnamate (EC).

Cinnamic acid ester derivate	*Melting point [°C]	*Boiling point [°C]	Density [g cm <sup>-3</sup> ]	Molecular weight [g mol <sup>-1</sup> ]	Molar volume [cm <sup>3</sup> mol <sup>-1</sup> ]
MC	36–38	254–255	1.092	162.188	148.524
IBC	–	287	1.003	204.269	203.658
AC	–	289–290	1.053	188.226	178.752
EC	6–7.5	271–272	1.047	176.215	168.305

\*At 760 mmHg.

glycol (PEG).<sup>[46]</sup> Some of the above-mentioned plasticizers are traditionally biobased, that is, citrates and tartrates, while others are petroleum-derived, that is, adipates and PEG, despite in the last years an alternative bio route has been developed for most of these plasticizers from biobased building blocks.<sup>[47,48]</sup> With the increasing concern about the environment, new biobased plasticizers for PLA are being sought with the aim of contributing to more sustainable development and enhancing ductile properties of PLA-based polymers.<sup>[32]</sup> have reported a systematic study of the features an organic plasticizer must reach to be efficient. They identified three main building blocks in designing organic plasticizers, each one contributing to a particular feature. They concluded the important role of aliphatic chains, ester groups, and aromatic rings to bring chain mobility, cohesion, and compatibility, respectively. By taking into account these building blocks, they suggested several biobased plasticizer candidates including cinnamates, *p*-coumarates, coumarin-3-carboxylic acid esters, and 2,5-furandicarboxylic acid esters. Thus, the main aim of this work is to assess, for the first time, the potential of different cinnamate esters, namely methyl trans-cinnamate (MC), isobutyl cinnamate (IBC), allyl cinnamate (AC), and ethyl cinnamate (EC), for PLA plasticization. The effect of varying the carboxylic acid chain length of esterified cinnamic acid at a constant concentration of 20 wt% on mechanical, thermal, thermo-mechanical, morphology, and biodegradation is shown in this work.

## 2. Experimental Section

### 2.1. Materials

The PLA used was supplied by Total Energies Corbion (Gorinchem, The Netherlands). The PLA is a commercial semi-

crystalline grade, reference Luminy L130. According to the supplier, this PLA grade has a density of 1.24 g cm<sup>-3</sup>. Different cinnamates, namely EC, MC, IBC, and AC were supplied by Sigma-Aldrich (Steinheim, Germany). **Figure 1** shows a schematic representation of the chemical structure of the different cinnamates used as plasticizers for PLA while **Table 1** gathers the main physicochemical properties of all four cinnamates.

### 2.2. Theoretical Solubility Parameters

Theoretical miscibility between PLA and the different proposed cinnamate plasticizers by calculating their corresponding solubility parameters ( $\delta$ ). The closer the values of these parameters, the higher the expected miscibility.<sup>[49]</sup> The solubility parameters of neat PLA and the different plasticizers (MC, IBC, AC, and EC) were obtained by the group contribution method proposed by Hoftyzer and Van Krevelen. This method allows the calculation of the three main components of the solubility parameter, which include the dispersive forces ( $\delta_d$ ), the polar forces ( $\delta_p$ ), and the hydrogen bonding forces ( $\delta_h$ ). The global solubility parameter ( $\delta$ ) results from the sum of these three contributions as indicated in Equation (1).<sup>[50]</sup>

$$\delta = \sqrt{\delta_d^2 + \delta_p^2 + \delta_h^2} \quad (1)$$

where

$$\delta_d = \frac{\sum F_{di}}{V_m} \quad (2)$$

$$\delta_p = \frac{\sqrt{\sum F_{pi}^2}}{V_m} \quad (3)$$

$$\delta_h = \sqrt{\frac{\sum E_{hi}}{V_m}} \quad (4)$$

$$\delta_v = \sqrt{\delta_d^2 + \delta_p^2} \quad (5)$$

Following the Hoftyzer–Van Krevelen method, it is possible to make a rather accurate value of the dispersive and polar forces contributions,  $\delta_d$ , and  $\delta_p$ , respectively (see Equations (2) and (3)). Nevertheless, the F-method cannot be used to estimate the contribution of hydrogen bonding. Despite this, as observed by Hansen, the cohesive energies of the different chemical groups are almost constant, and therefore, it is possible to estimate the hydrogen bonding contribution ( $\delta_h$ ) by the cohesive energy group contribution<sup>[51]</sup> (Equation 4). In addition, Bagley et al.<sup>[52]</sup> proposed the calculation of a  $\delta_v$  parameter, which relates the dispersive and polar contributions ( $\delta_d$ ,  $\delta_p$ ) as they have the same impact on solubility (Equation (5)). By assigning the parameters  $\delta_d$ ,  $\delta_p$ , and  $\delta_h$  to a spatial coordinate system (x, y, z), it is possible to obtain a 3D solubility diagram of a particular polymer, which is defined by a spherical region (Hansen space) with the center located at ( $\delta_d$ ,  $\delta_p$ ,  $\delta_h$ ). The solubility sphere of a particular polymer has a radius ( $R_0$ ) that can be obtained experimentally and defines the solubility threshold. For PLA, the solubility sphere ( $R_0$ ) is 10.7 MJ m<sup>-3</sup> as Auras et al. reported.<sup>[53]</sup> A 2D representation of the Hansen space can be obtained by plotting a circle centered at ( $\delta_h$ ,  $\delta_v$ ). In this case, if the solubility parameter coordinates ( $\delta_h$ ,  $\delta_v$ ) of a plasticizer fall inside the circle, then, good miscibility could be expected.<sup>[54]</sup> A numerical approach to the potential miscibility can be obtained from the relative by using Equation (6) which takes the form of the Euclidean 3D distance between two points.

$$R_a = \sqrt{4 \left( \delta_{d\_plast} - \delta_{d\_PLA} \right)^2 + \left( \delta_{p\_plast} - \delta_{p\_PLA} \right)^2 + \left( \delta_{h\_plast} - \delta_{h\_PLA} \right)^2} \quad (6)$$

Equation (7) gives the relative energy difference (RED). RED determines the distance between  $R_a$  and  $R_0$ . If  $R_0$  is greater than the solubility parameter distance ( $R_a$ ), then the plasticizer's good solubility could be expected. Therefore, if  $RED < 1$ , there is good solubility; otherwise, if  $RED \geq 1$ , the compounds will not exhibit good affinity.

$$RED = \frac{R_a}{R_0} \quad (7)$$

### 2.3. Processing of Plasticized PLA Formulations

Before processing, PLA was subjected to a drying process at 65 °C for 48 h in an oven to prevent PLA from hydrolysis. Subsequently, all formulations were weighed and homogenized by

manual methods. All plasticized formulations contained 80 wt% PLA and 20 wt% cinnamate plasticizers. The following coding PLA-XX, was used where XX refers to the corresponding cinnamate, namely -MC, -IBC, -AC, and -EC.

The PLA/cinnamate ester mixtures were compounded in a twin-screw co-rotating extruder supplied by Dupra S.L. (Alicante, Spain). The temperature profile was set by taking into account the melting temperature ( $T_m$ ) of a semi-crystalline PLA. The four-barrel heating stages were programmed (from the feed hopper to the nozzle) at 170–175–180–185 °C and a rotation speed of 25 rpm was used for all formulations. The compounded strands were cooled down to room temperature and subsequently pelletized using an air knife. Standardized pieces for tensile (bone shape) and impact (Charpy) tests were obtained by injection molding in a Meteor 270/75 from Mateu & Solé (Barcelona, Spain). The temperature profile was set to 200 °C in the feeding hopper, 195 °C in the screw zone, and 185 °C in the injection nozzle. The injection time was set as 1 s and pressure was kept for 30 s to ensure the correct quality of the samples.

### 2.4. Characterization of Plasticized PLA Formulations

#### 2.4.1. Mechanical Properties

The mechanical properties of neat PLA and plasticized formulations containing esters of cinnamic acid were obtained in terms of tensile, impact strength (Charpy test), and Shore D hardness. Tensile tests were carried out in an ELIB 30 universal testing machine provided by Ibertest (Madrid, Spain). The test conditions and the specimens (dog-bone shape) followed ISO 527. A 5 kN load cell with a crosshead speed of 10 mm min<sup>-1</sup> was used to obtain the main tensile parameters. The test was carried out on five different specimens of each formulation to obtain reliable results, and the corresponding tensile parameters were averaged. The impact strength test was carried out in a 6-J Charpy pendulum from Metrotec (San Sebastian, Spain) as recommended by ISO 179. At least five specimens of each formulation were tested, and the obtained impact strength values were averaged. With regard to hardness, Shore D hardness was measured at room temperature in a durometer model 673-D provided by J. Bot S.A. (Barcelona, Spain), following ISO 868, with a stabilization time of 15 s. This procedure was performed at five different points for each formulation.

#### 2.4.2. Morphological Characterization

The morphological characterization of the fracture surfaces of PLA and plasticized PLA formulations with esters of cinnamic acid. To this, broken samples from impact tests were observed by field emission scanning electron microscopy (FESEM). A ZEISS ULTRA 55 FESEM microscope from Oxford Instruments (Abingdon, UK) operated at 2 kV was used. Before FESEM observation, the samples' surfaces were coated by an ultrathin gold-palladium layer in a high vacuum sputter coater EM MED20 provided by Leica Microsystem (Milton Keynes, UK).

#### 2.4.3. Thermal Properties

The main thermal transitions of neat PLA and the plasticized formulations with cinnamates were obtained by differential scan-

**Table 2.** Summary of the theoretical solubility parameters, distance, and RED values according to the Hoftyzer–Van Krevelen group contribution method of polylactide (PLA) and different cinnamic acid esters.

	$\delta_d$ [MJ m <sup>-3</sup> ] <sup>1/2</sup>	$\delta_p$ [MJ m <sup>-3</sup> ] <sup>1/2</sup>	$\delta_h$ [MJ m <sup>-3</sup> ] <sup>1/2</sup>	$\delta$ [MJ m <sup>-3</sup> ] <sup>1/2</sup>	$\delta_v$ [MJ m <sup>-3</sup> ] <sup>1/2</sup>	$R_a$	RED
PLA	15.33	8.44	10.98	20.66	17.50	–	–
Methyl trans-cinnamate	17.78	3.38	6.87	19.36	18.10	8.16	0.76
Isobutyl cinnamate	16.73	2.46	5.86	17.90	16.91	8.36	0.78
Allyl cinnamate	17.11	2.81	6.26	18.43	17.34	8.16	0.76
Ethyl cinnamate	17.29	2.98	6.45	18.69	17.54	8.11	0.76

ning calorimetry (DSC). The tests were performed on samples with a mass of  $\approx 7$  mg under a nitrogen atmosphere (66 mL min<sup>-1</sup>) in a modulated heat flow DSC model Q2000 from TA instruments (New Castle, Delaware, USA). The samples were subjected to a dynamic program with three steps. The first heating cycle was carried out to remove the thermal history resulting from the previous processing (injection molding). This heating step was scheduled from 30 to 180 °C. After this, a cooling step down to  $-50$  °C was programmed. Finally, the samples were subjected to a second heating step from  $-50$  °C up to 220 °C. The heating/cooling rate for all three steps was 10 °C min<sup>-1</sup>. The main thermal parameters, such as the glass transition temperature ( $T_g$ ), the melt peak temperature ( $T_m$ ), the enthalpy of fusion ( $\Delta H_m$ ), the cold crystallization peak temperature ( $T_{cc}$ ), and the cold crystallization enthalpy ( $\Delta H_{cc}$ ), were obtained from the second heating cycle. In addition, the percentage degree of crystallinity ( $\chi_c\%$  and  $\chi_{c,max}\%$ ) was obtained by using Equations (8) and (9).

$$\chi_c = \frac{\Delta H_m - \Delta H_{cc}}{\Delta H_m^0 \cdot w} \quad (8)$$

$$\chi_{c,max} = \frac{\Delta H_m}{\Delta H_m^0 \cdot w} \quad (9)$$

where  $\Delta H_m^0$  corresponds to the theoretical melting enthalpy of fully crystalline PLA (93 J g<sup>-1</sup>),<sup>[55]</sup> and  $w$  is the PLA weight fraction.

The thermal stability at high temperatures and degradation of neat PLA and plasticized PLA formulations were studied by thermogravimetric analysis (TGA) on a Mettler–Toledo TGA/SDTA 851 thermobalance (Schwerzenbach, Switzerland). The test was performed on samples with an average mass of  $\approx 15$  mg. The samples were subjected to a heating program from 30 to 700 °C at a constant heating rate of 10 °C min<sup>-1</sup> under a nitrogen atmosphere (flow rate of 66 mL min<sup>-1</sup>).

#### 2.4.4. Dynamic-Mechanical Thermal Analysis

The dynamic-mechanical thermal behavior of PLA and the plasticized formulations with different esters of cinnamic acid was studied by dynamic mechanical thermal analysis (DMTA). The analysis was performed on a dynamic analyzer model DMA1 from Mettler–Toledo (Schwerzenbach, Switzerland), working on simple cantilever/bending conditions with rectangular samples of dimensions 20 × 7 × 1 mm<sup>3</sup>. These samples were heated from

0 to 110 °C at a heating rate of 2 °C min<sup>-1</sup>. The frequency and maximum bending deflection were 1 Hz and 0.1%, respectively.

## 3. Results and Discussion

### 3.1. Theoretical Approach to Miscibility of PLA and Cinnamates

**Table 2** gathers a summary of the total solubility parameters ( $\delta$ ) and their contributions ( $\delta_d$ ,  $\delta_p$ , and  $\delta_h$ ) for neat PLA and all potential plasticizers from cinnamic acid esters. Neat PLA has a  $\delta$  parameter of 20.66 (MJ m<sup>-3</sup>)<sup>1/2</sup> which agrees with values reported in the literature.<sup>[56–58]</sup> The solubility parameters of the four cinnamates considered as potential plasticizers for PLA range between 17.90 and 19.36 (MJ m<sup>-3</sup>)<sup>1/2</sup> with methyl trans-cinnamate being the closer to PLA. In general, these solubility parameters are close to that of PLA, and therefore, good miscibility should be expected. This miscibility can be quantified by RED, which ranges between 0.76 and 0.78. Since these RED values for all four cinnamates considered in this study are below 1, good miscibility is expected since all these cinnamates fall inside the solubility sphere of PLA. Similar results have been reported by Aliotta et al.<sup>[54]</sup> in PLA, PBAT, and PLA/PBAT blends. They observed a RED value of 0.76 between PLA and acetyl tributyl citrate (ATBC) plasticizer, thus suggesting a good affinity between them. By representing Bagley's diagram, the good affinity between all four cinnamates and PLA is also evident (**Figure 2**), since their solubility parameter coordinates ( $\delta_v$  and  $\delta_h$ ) fall inside the solubility region of PLA.<sup>[52]</sup>

### 3.2. Quantification of the Actual Plasticizer Content after Processing

Despite all used cinnamates having a high boiling point (above 250 °C), monomeric plasticizers are much more volatile than polymeric plasticizers. Llanes et al.<sup>[59]</sup> reported this phenomenon on plasticized PLA formulations with dibutyl maleate (DBM) and dibutyl fumarate (DMF), with a boiling point of 281 and 280 °C, respectively, they observed some plasticizer loss during processing at temperatures ranging from 160 to 170 °C. Despite this plasticizer loss, they reported exceptional plasticization properties of these two biobased plasticizers by reaching elongation at break values of 220% and 120%, for plasticized formulations with 12 wt% DBF and DMF, respectively. Thermogravimetry is very useful to measure the actual plasticizer content after processing since the monomeric plasticizer is removed at lower temperatures than the polymer as can be seen in **Figure 3**. By measuring

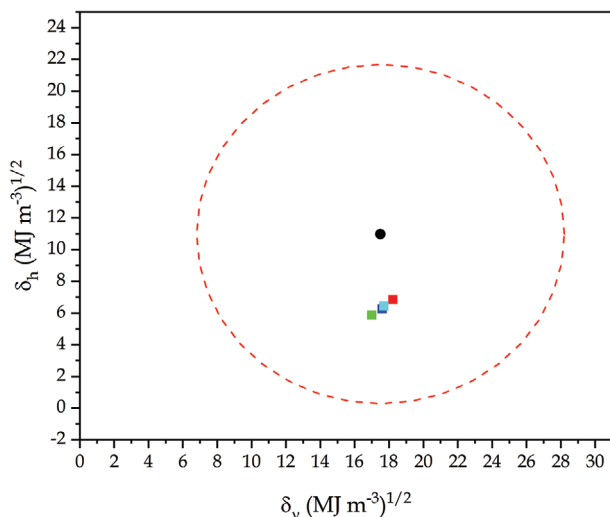


**Figure 2.** Bagley's solubility diagram of PLA and different methyl trans-cinnamate (■ MC), isobutyl cinnamate (■ IBC), allyl cinnamate (■ AC), and ethyl cinnamate (■ EC).

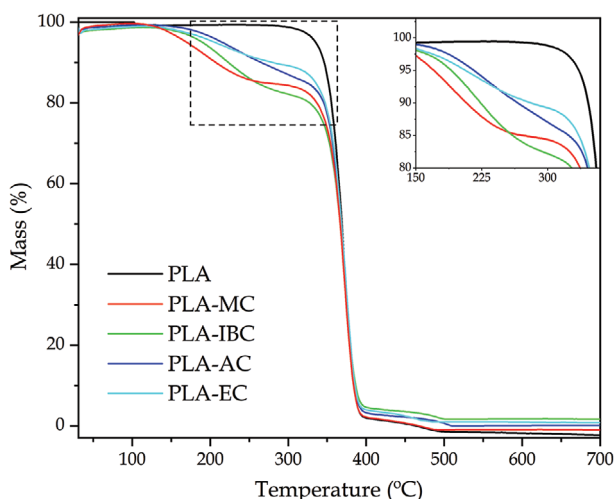


**Figure 3.** Comparative TGA plots of neat PLA and plasticized PLA formulations containing 20 nominal wt% of cinnamic acid esters.

the weight loss in this stage, it is possible to obtain the actual content of the different cinnamates after processing. **Table 3** gathers the weight loss at 300 °C (first degradation stage) and the actual plasticizer content, as well as the percentage loss of each cinnamate.

As can be seen, PLA degrades in a single step with an onset degradation temperature of 335.7 °C according to its TGA thermogram, and a maximum degradation rate temperature of 372–373 °C. This stage comprises the temperature range between 320 and 400 °C and represents a weight loss of more than 95%, which is related to chain scission through ester groups as Agüero et al. proposed.<sup>[60]</sup> A second (and almost negligible) stage can be observed at temperatures comprised between 420 and 500 °C, which promotes the total degradation of the residual backbone, and char formation. With regard to plasticized PLA formulations with cinnamates, the characteristic TGA degradation

**Table 3.** Summary of thermal parameters obtained by thermogravimetry (TGA) tests of neat PLA and plasticized PLA formulations containing 20 wt% of cinnamic acid esters.

Code	Nominal plasticizer content [wt%]	Mass loss at 300 °C [%]	Plasticizer loss [%]	$T_{deg}$ [°C]
PLA	–	–	–	370.7 ± 4.6
PLA-MC	20	17.7 ± 0.3	11.5 ± 1.5	373 ± 7.5
PLA-IBC	20	18.6 ± 0.4	7 ± 2.0	373 ± 6.3
PLA-AC	20	14.3 ± 0.9	28.5 ± 4.5	370.7 ± 4.2
PLA-EC	20	10.9 ± 0.7	45.5 ± 3.5	373 ± 7.0

curve shows remarkable differences. In particular, a first stage, comprised between 200 and 300 °C is observed, which is attributable to the plasticizer loss as monomeric plasticizers are more volatile than polymeric plasticizers. This phenomenon has also been observed by Arrieta et al.<sup>[61]</sup> in plasticized PLA formulations containing 15 wt% limonene (with a boiling point of 176–177 °C). TGA results showed some plasticizer was lost during processing at 180 °C for 5 min. Despite they used a nominal wt% limonene of 15% and 20%, the residual plasticizer after processing was 6.5% and 8.5%, respectively, which represents a percentage loss of 56.7%, and 57.5% for the composition containing a nominal limonene content of 15% and 20%, respectively. Martino et al.<sup>[62]</sup> observed this plasticizer loss in plasticized PLA with a monomeric plasticizer, namely, dioctyl adipate (DOA), while this phenomenon was almost negligible in some polymeric polyadipates, thus corroborating the sensitiveness of monomeric plasticizers to volatilization during thermal processing.

In this work, the maximum plasticizer loss is obtained for ethyl cinnamate with a weight loss of 45.5% while the minimum plasticizer loss is detected for IBC. These results are similar to those reported previously with other monomeric plasticizers, and as observed by Llanes et al.,<sup>[59]</sup> this loss does not compromise the plasticization efficiency, especially with high nominal plasticizer content. Despite TGA has revealed some plasticizer loss attributable to processing conditions, the code used in this manuscript will include the nominal wt% (20 wt%), while the actual plasticizer content obtained from **Table 3** will be used to calculate some thermal properties, in particular, the normalized enthalpies to estimate the degree of crystallinity.

### 3.3. Mechanical Properties of Plasticized PLA with Cinnamates

The main mechanical properties obtained by tensile, Charpy, and Shore D hardness tests are gathered in **Table 4** while **Figure 4** shows a comparative plot of the curves. Neat PLA shows its typical brittle behavior with a tensile modulus and strength of 2427.7 and 52.7 MPa, respectively. It is worthy to note its low elongation at a break of 3.9% which confirms its low toughness and brittleness as proposed by Tejada-Oliveros et al.<sup>[63]</sup> In general, cinnamates provide interesting plasticization properties to PLA, except for the plasticized formulation with ethyl cinnamate. As can be seen in **Table 4**, the plasticized PLA formulations containing 20 wt% of MC, IBC, and AC are less rigid as their corresponding tensile moduli, in the 997–1323 MPa range suggest. Accordingly,

**Table 4.** Summary of the mechanical properties (tensile properties, Shore D hardness, and impact strength) of neat PLA and plasticized PLA formulations containing 20 wt% of cinnamic acid esters.

Code	Tensile properties			Shore D hardness	Impact strength [kJ m <sup>-2</sup> ]
	Elastic modulus, $E_t$ [MPa]	Strength, $\sigma_t$ [MPa]	Elongation at break, $\epsilon_b$ [%]		
PLA	2427.7 ± 63.6	52.7 ± 1.4	3.9 ± 0.3	61.6 ± 1.3	3.9 ± 0.2
PLA-MC	1322.9 ± 96.8	21.5 ± 1.3	285 ± 13.6	57 ± 0.9	4.1 ± 0.3
PLA-IBC	1103.8 ± 101.6	17.4 ± 0.9	250 ± 8.8	54.7 ± 0.8	4.8 ± 0.3
PLA-AC	996.9 ± 102.8	14.6 ± 0.7	339.4 ± 15.7	54.7 ± 0.5	5.6 ± 0.4
PLA-EC	2421.4 ± 77.3	34.6 ± 1.9	2.8 ± 0.1	61.63 ± 1.7	3.5 ± 0.2

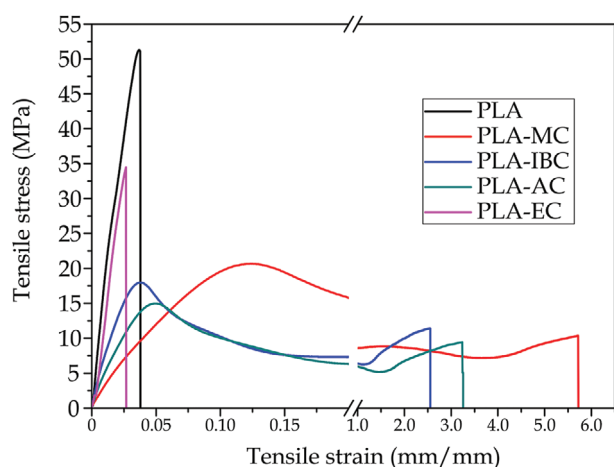


**Figure 4.** Comparative tensile test of neat PLA and plasticized PLA formulations containing 20 nominal wt% of cinnamic acid esters.

the tensile strength of the plasticized PLA formulations is smaller with values ranging from 14.6 (PLA-AC) up to 21.5 MPa (PLA-MC). The reduction in strength is a typical effect with the incorporation of a plasticizer, as many other researchers propose.<sup>[64,65]</sup> This effect is associated with the increased chain mobility that promotes the breakage of the sample with lower tensile strength. Another factor to consider is that the tensile strength of most of the most commonly used polymers is in the 20–35 MPa range.<sup>[66]</sup>

The most astonishing effect is the increase in the elongation at break which changes from 3.9% (neat PLA) up to values above 250% with MC, IBC, and AC. This confirms the exceptional plasticization efficiency of these three cinnamic acid esters, namely MC, IBC, and AC. Since PLA is a polyester, the presence of ester groups in cinnamates positively contributes to establishing hydrogen bonding thus improving their affinity.<sup>[32,67]</sup> These results are very promising and comparable to those reported by Arrieta et al.<sup>[68,69]</sup> in plasticized PLA films containing 15 wt% ATBC, with an elongation at break in the 180–225% range. With regard to EC, the mechanical properties suggest poor plasticization efficiency since the tensile modulus is almost identical to that of neat PLA and the elongation at break is not improved; in fact, it is lower than neat PLA. Despite the theoretical approach to solubility indicating EC was a good candidate for PLA plasticization, as indicated previously, the actual amount of remaining EC in PLA is the lowest of all four cinnamates (10.9 wt%), which seems to be insuf-

ficient to trigger the plasticization mechanisms. This is reflected in poor mechanical properties as observed by Kasmi et al.,<sup>[65]</sup> in plasticized PLA with ferulic acid derivatives. This threshold to trigger the plasticization properties has been described by Murariu et al.,<sup>[70]</sup> in PLA plasticized with increasing content of glyceryl triacetate (GTA), and tributyl *O*-acetyl citrate (TBAC). They observed that the nominal strain at break of neat PLA (11%) was not improved by the addition of 10 wt% GTA or TBAC with nominal strain values of 11% and 8%, respectively. Nevertheless, the nominal strain at break was surprisingly higher by the addition of 15 wt% of GTA or 15 wt% TBAC, which suggested a plasticizer threshold is needed to obtain clear evidence of plasticization, and obviously, it depends on the compound.

With regard to the impact strength, this is directly related to toughness. As depicted in Table 4, neat PLA has an impact strength of 3.9 kJ m<sup>-2</sup>; once again, all plasticized PLA formulations with cinnamates, except that with ethyl cinnamate, offer increased impact strength, thus giving evidence of improved toughness. The plasticized formulation with allyl cinnamate shows an impact strength of 5.6 kJ m<sup>-2</sup>, which is remarkably higher than that of neat PLA. As tensile properties suggested, ethyl cinnamate does not improve the impact strength but a slight decrease is obtained. In this case, ethyl cinnamate provides an anti-plasticization effect as reported in the literature in plasticized polymers with low amounts of plasticizers, below a certain threshold as proposed by Jacobsen et al.<sup>[71]</sup> Other authors have reported the implementation of different strategies to improve the toughness of PLA by the introduction of nucleating agents or by blending with other polymers.<sup>[72,73]</sup> The Shore D hardness follows the same tendency observed in tensile properties regarding modulus. Once again, all cinnamates except for ethyl cinnamate, give low Shore D hardness values thus indicating good plasticization.

### 3.4. Morphology of Fracture Surface of Plasticized PLA with Cinnamates

The morphology of the fractured samples after the impact test was studied by FESEM (Figure 5). Figure 4a shows the typical brittle fracture of neat PLA with a smooth and flat surface which is representative of low (or almost absence) plastic deformation as suggested by Gonzalez et al.<sup>[55]</sup> Plasticization with methyl trans-cinnamate, IBC, and allyl cinnamate leads to a noticeable change in surface morphology. Figures 4b and 4c show the mor-

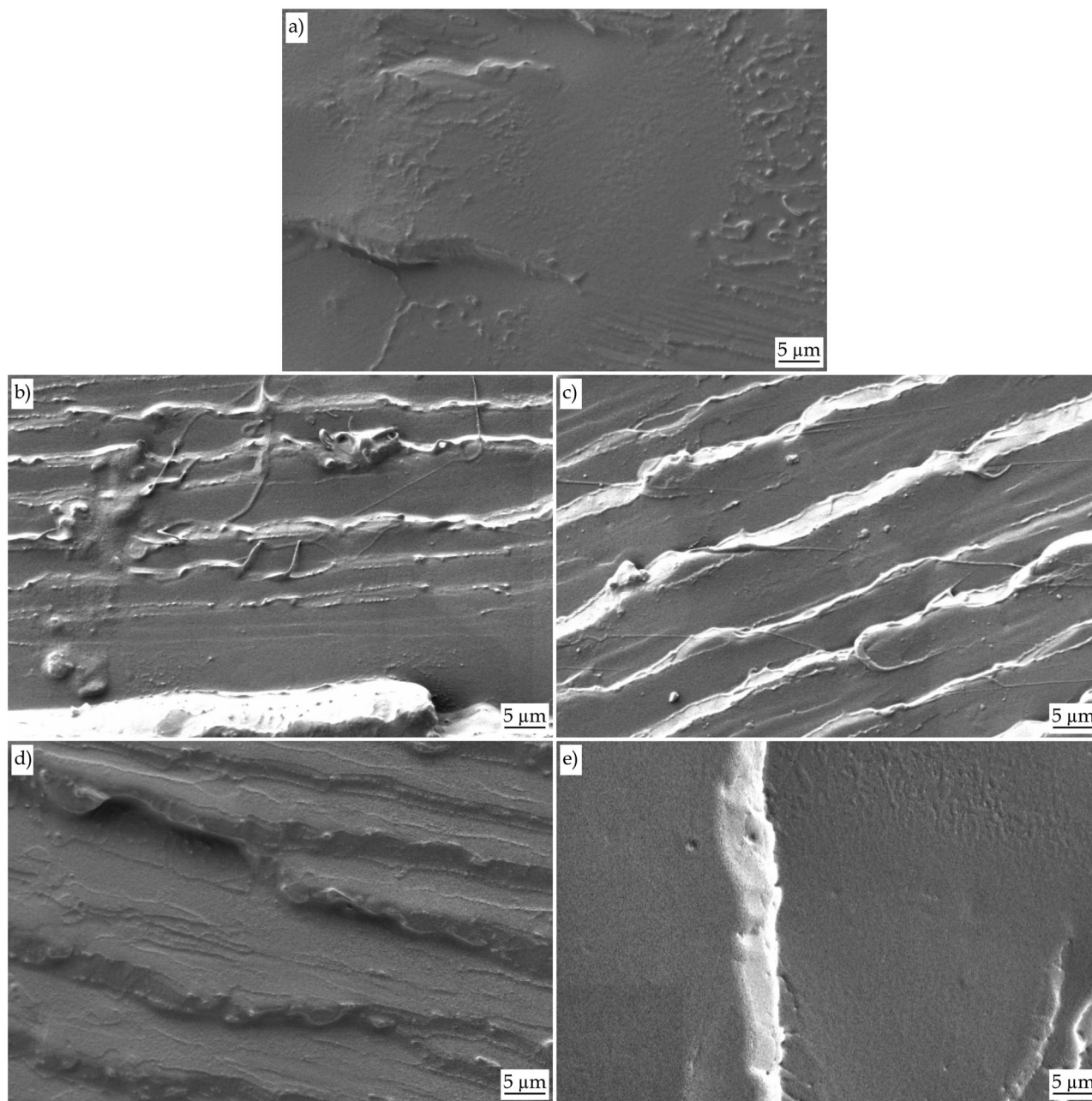


**Figure 5.** Field emission scanning electron microscopy (FESEM) images of the fracture surface of specimens after Charpy's impact test of a) neat PLA, b) PLA-MC, c) PLA-IBC, d) PLA-AC, and e) PLA-EC. Images were taken at 1000 $\times$ , with a marker scale of 5  $\mu\text{m}$ .

phology of the fractured surface of PLA-MC and PLA-IBC, respectively. These images show some filaments and a rough and heterogeneous surface which are representative of plastic deformation. This morphology confirms the obtained mechanical properties. Similar morphology was described by Rojas-Lema et al.,<sup>[45]</sup> in plasticized PLA with OLA. This rough surface is even more pronounced in PLA-AC (Figure 4d) with a wavy rough surface related to increased ductile behavior. The incorporation of an effective plasticizer also contributes to reducing microcrack formation and growth since no microcracks can be observed in Figure 4b–d. This behavior has been reported by Lascano et al.<sup>[74]</sup> in plasti-

cized PLA with OLA with a particular increase in impact strength related to plastic deformation. Regarding the surface morphology of the plasticized PLA formulation with ethyl cinnamate (Figure 4e), it can be clearly distinguished the typical brittle flat surface, which is in accordance with the observed mechanical properties. This morphology agrees with the previous TGA characterization that revealed the lowest remaining plasticizer for ethyl cinnamate. It is worth noting the absence of phase separation in all four cinnamate-plasticized PLA formulations. If phase separation occurs due to restricted miscibility, a second phase, usually with a spherical shape, appears. This effect has been described

**Table 5.** Summary of the main thermal parameters obtained by DSC tests of neat PLA and plasticized PLA formulations containing 20 wt% of cinnamic acid esters.

Code	$T_g$ [°C]	$T_m$ [°C]	$\Delta H_m$ [J g <sup>-1</sup> ]	$T_{cc}$ [°C]	$\Delta H_{cc}$ [J g <sup>-1</sup> ]	$\chi_c$ [%] <sup>a)</sup>	$\chi_{c,max}$ [%] <sup>b)</sup>
PLA	61.7 ± 1.2	168.4 ± 3.4	17.5 ± 0.4	113.4 ± 2.3	4.9 ± 0.1	13.5 ± 0.3	18.8 ± 0.4
PLA-MC	47.4 ± 0.5	163.6 ± 2.5	29.8 ± 0.5	92.6 ± 1.9	22.7 ± 0.4	9.3 ± 0.2	38.9 ± 0.7
PLA-IBC	44 ± 0.9	164 ± 3.3	29.6 ± 0.4	89.3 ± 1.4	22.7 ± 0.5	9.1 ± 0.2	39.1 ± 0.5
PLA-AC	36.1 ± 0.5	159.9 ± 3.2	33 ± 0.3	85.3 ± 1.7	23.1 ± 0.4	12.4 ± 0.2	41.4 ± 0.4
PLA-EC	56.8 ± 1.1	167.3 ± 1.7	32.3 ± 0.7	97.3 ± 1.6	21.7 ± 0.4	12.8 ± 0.4	39.0 ± 0.9

<sup>a)</sup>  $\chi_c$  stands for the degree of crystallinity of injection molded samples; <sup>b)</sup>  $\chi_{c,max}$  stands for the maximum degree of crystallinity reached by samples after heating in DSC.

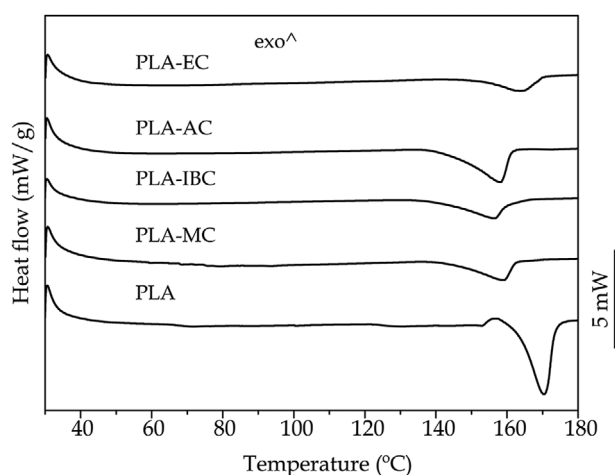


**Figure 6.** Differential Scanning Calorimetry (DSC) thermograms of the second heating step for PLA and plasticized PLA formulations containing 20 wt% of cinnamic acid esters.

by Ferri et al.<sup>[44]</sup> in plasticized PLA with epoxidized fatty acid esters (EFAE). Above 4.7 wt% EFAE, plasticizer saturation occurs, thus leading to a phase separation phenomenon that also has a negative effect on mechanical properties. This phenomenon cannot be observed in Figure 4, thus suggesting the good affinity of PLA with all cinnamates, independently of their plasticization efficiency, as the theoretical study of the solubility parameters indicated.

### 3.5. Thermal Properties of Plasticized PLA with Cinnamates

Table 5 gathers the main thermal properties obtained by DSC and Figure 6 the thermogram's representation.

As previously indicated, one of the main aims of incorporating plasticizers is to provide improved flexibility or ductility. The plasticizer efficiency can be assessed by the decrease in the glass transition temperature ( $T_g$ ) it provides. As the  $T_g$  decreases, chain mobility is favored and hence, mechanical ductile properties are improved in Murariu et al. work.<sup>[70]</sup> All four cinnamate lead to a decrease in the glass transition temperature of neat PLA, which is located at 61.7 °C. In accordance with the previously reported mechanical properties, allyl cinnamate gave the maximum elongation at the break on plasticized PLA (339.4%). These results are with the observed  $T_g$  values since PLA-AC has the lowest

$T_g$  of all plasticized PLA formulations, with a value of 36.1 °C. IBC and methyl trans-cinnamate also give a noticeable decrease in  $T_g$ , with values of 44 and 47.4 °C, respectively, thus showing their good plasticization efficiency. With regard to ethyl cinnamate, it also provides a decrease in  $T_g$  but not as high as those observed with the other cinnamates which agree with the lowest plasticizer content. This noticeable decrease in  $T_g$  is due to the insertion of low molecular weight cinnamate molecules between the PLA chains in the amorphous regions, with a subsequent increase in the free volume and a weakening of the polymer chain-to-polymer chain intermolecular interactions, which in turn, provide increase chain mobility.<sup>[75–77]</sup> Despite Llanes et al.<sup>[59]</sup> reported a noticeable decrease in  $T_g$  of neat PLA from 58 °C down to 35 and 22 °C for DBM (12 wt% DBM), and DMF (12 wt% DBF), respectively, the obtained values for elongation at break were 111.9% and 210% for the plasticized PLA formulation with DBM and DBF, respectively. On the other hand, despite the  $T_g$  of plasticized PLA formulations containing 7 wt% DBM and DBF being significantly lower, namely 37 and 40 °C, respectively, the plasticization efficiency, in terms of ductile properties, was very poor, with very low elongation at break values (<3%), thus suggesting there is a threshold to provide good plasticization. In fact, this situation is similar to that obtained in this study with ethyl cinnamate, which provides a moderate decrease in  $T_g$ , while mechanical ductile properties were not improved.

The plasticization efficiency is also evidenced by a shift of the cold crystallization peak ( $T_{cc}$ ) to lower temperatures. The  $T_{cc}$  for neat PLA is 113.4 °C and, in agreement with the  $T_g$  values, allyl cinnamate-plasticized PLA formulations give the lowest  $T_{cc}$  value of 85.3 °C. Tábi et al.<sup>[78]</sup> reported PLA is a polymorphic polymer with four different crystal types:  $\alpha$ ,  $\beta$ ,  $\gamma$ ,  $\epsilon$ , and a disordered crystal form,  $\alpha'$ . Despite  $\alpha$ -crystals being developed from the melt at temperatures above 120 °C, the  $\alpha'$ -crystals are obtained at temperatures below 100 °C. A mixture of  $\alpha$ - and  $\alpha'$ -crystals is obtained in the 100–120 °C range. Since the  $T_{cc}$  changes from 113.4 °C for neat PLA to values lower than 100 °C for all four cinnamates, a change in the crystal-type formation is expected. Baiardo et al.<sup>[79]</sup> reported this noticeable decrease in  $T_{cc}$  in plasticized PLA formulations containing ATBC and different molecular weight PEGs.

As indicated by Shi et al.,<sup>[80]</sup> the degree of crystallinity in PLA developed under conventional processing techniques is relatively low. This low crystallization rate results in a low degree of crystallinity,  $\chi_c$ %. In this work, neat PLA shows a  $\chi_c$ % of 13.5% after the injection molding process (calculated by subtracting the cold crystallization peak enthalpy,  $\Delta H_{cc}$  to the melt peak crystallization enthalpy,  $\Delta H_m$ ) and cannot reach much more crystallinity



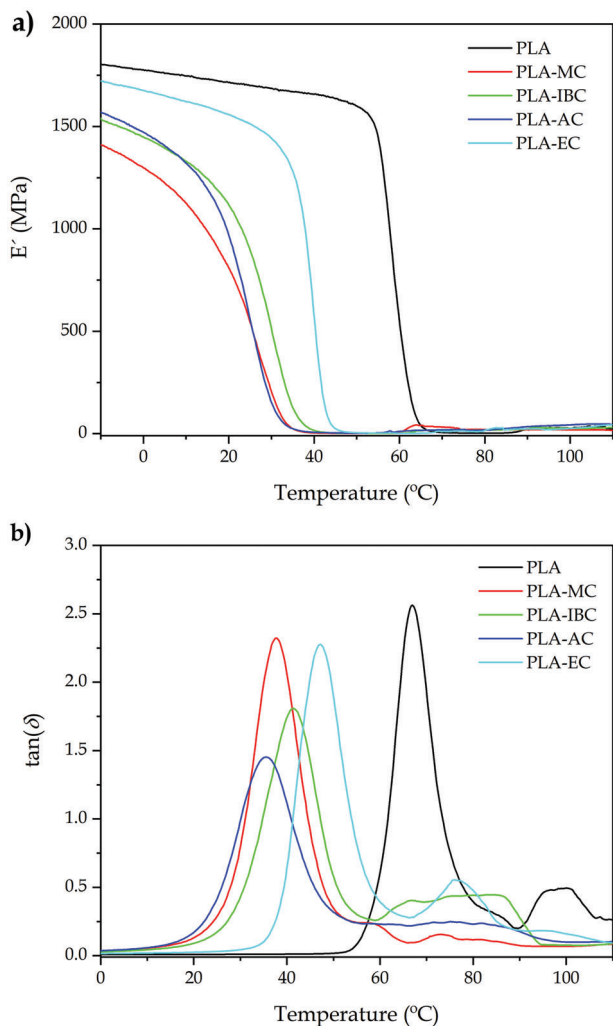


**Figure 7.** Comparative plots of the evolution of a) storage modulus,  $E'$  and b) dynamic damping factor,  $\tan \delta$ , as a function of the temperature of neat PLA and plasticized PLA formulations containing 20 wt% of cinnamic acid esters.

after heating as indicated by its  $\chi_{c,max}$  % of 18.8% (calculated considering only the melt peak crystallization which includes the degree of crystallinity developed during processing plus the cold crystallization contribution). Plasticizers have an effect on crystallinity, as observed in Table 5 with the addition of plasticizers. The presence of any of the four cinnamates considered in this

study leads to a noticeable increase in the maximum degree of crystallinity that can be developed after processing plus cold crystallization, reaching values around 40%. These results agree with those reported by Xiao et al.<sup>[81]</sup> on plasticized PLA with triphenyl phosphate (TPP). They observed a  $\chi_c$  % of 13.8% for neat PLA, which was almost the maximum since they did not observe cold crystallization. The addition of TPP in the 10–30 wt% range led to a remarkable increase in the crystallinity developed during cold crystallization, up to values in the 26–30% range, and in a parallel way, the maximum degree of crystallinity increases in a remarkable way up to values ranging from 43.8% to 52.5% for 10 wt% TPP and 30 wt% TPP, respectively.

### 3.6. Dynamic-Mechanical Thermal Properties of Plasticized PLA with Cinnamates

Figure 7 shows the DMTA behavior of neat PLA and all four plasticized formulations containing 20 wt% of different cinnamates. Moreover, Table 6 gathers some useful information obtained by DMTA. Figure 5a shows the plot comparison of the storage modulus ( $E'$ ) as a function of increasing temperature. As it can be clearly seen, plasticization with all four cinnamates leads to a shift of the storage modulus curve to lower temperatures due to the increased chain mobility. Another typical effect of plasticization on DMTA behavior is a decrease in  $E'$  all along the considered temperature range. While neat PLA shows an  $E'$  value of 1714.3 MPa, plasticization with methyl trans-cinnamate and allyl cinnamate gives half the values of neat PLA, 812.8 and 965.8 MPa, respectively. Once again, the effect of ethyl cinnamate stands out. As previously indicated, the actual amount of this plasticizer contained in PLA is lower than other cinnamates, and therefore, its plasticization effects are less intense. This low plasticization efficiency of ethyl cinnamate can be seen in Figure 7a, since the shift of the  $E'$  versus  $T$  curve toward lower temperatures is less pronounced than those obtained with the other cinnamates. Accordingly, PLA-EC is stiffer than other PLA-cinnamate formulations; in fact, its  $E'$  value at 20 °C is slightly lower (1559.6 MPa) than neat PLA (1714.3 MPa). As mentioned above, plasticization with cinnamates provides increased chain mobility, thus allowing more ductility, and subsequently, less rigid materials are obtained. The plasticizer provides increased free volume and a weakening of the polymer chain-to-polymer chain interactions, which results in more ductile materials, with increased elongation ability as Harte et al. reported.<sup>[82]</sup> In this work, all four cinnamates promote a decrease in the temperature at which the  $\alpha$ -relaxation process takes place. This phenomenon is frequently associated with a glass transition temperature ( $T_g$ ) but it can be

**Table 6.** DMTA of neat PLA and plasticized PLA formulations containing 20 wt% of cinnamic acid esters.

Code	$T_\alpha^a$ [°C]	FWHM <sup>b</sup> [°C]	$\tan \delta$ peak maximum	$E'$ at 20 °C [MPa]	$E'$ at 50 °C [MPa]
PLA	67 ± 1.3	9.2 ± 0.5	2.57 ± 0.20	1714.3 ± 27.4	1598.3 ± 25.6
PLA-MC	37.8 ± 0.6	12.3 ± 1	2.34 ± 0.18	812.8 ± 13.0	2.2 ± 0.1
PLA-IBC	41.23 ± 0.6	14.4 ± 1.1	1.78 ± 0.24	1119.9 ± 15.7	2.4 ± 0.1
PLA-AC	35.63 ± 0.5	15.9 ± 1.4	1.42 ± 0.22	965.8 ± 14.5	3.1 ± 0.1
PLA-EC	47.26 ± 0.8	11.8 ± 1.2	2.29 ± 0.17	1559.6 ± 26.5	4.7 ± 0.1

<sup>a</sup>) The  $T_\alpha$  in DMTA has been calculated by using the  $\tan \delta$  peak maximum criterion; <sup>b</sup>) FWHM stands for the full-width at half-maximum of the  $\tan \delta$  peak.

also named a  $T_{\alpha}$ .<sup>[83]</sup> As can be seen in Figure 7a, neat PLA shows an almost constant storage modulus up to 50 °C. In the 50–70 °C range, the storage modulus decreases by three orders of magnitude. This dramatic decrease is related to the softening  $\alpha$ -relaxation process. Despite there are several criteria to assess the  $T_{\alpha}$  from DMTA data, one of the most used is the peak maximum of the dynamic damping factor ( $\tan \delta$ ), as observed in Figure 7b. By considering this criterion, neat PLA has a  $T_{\alpha}$  of 67 °C while all plasticized formulations with cinnamates show a noticeable decrease by reaching  $T_{\alpha}$  values below 50 °C. It is worthy to remark on the exceptionally low  $T_{\alpha}$  value allyl cinnamate provides to PLA, which agrees with the mechanical properties mentioned above. Despite the  $T_{\alpha}$  values by using the  $\tan \delta$  peak criterion being different from those obtained by the change in the heat capacity observed by DSC, they follow the same tendency. The lowest  $T_{\alpha}$  value measured by DSC was for allyl cinnamate (36.1 °C), and the  $T_g$  by DMTA for this plasticized formulation is the lowest (35.6 °C). It is worth noting that  $T_{\alpha}$  represents a change in the mechanical behavior from a rigid and stiff state to a rubbery-like state. By taking into account the  $T_{\alpha}$  of neat PLA (67 °C) and the  $T_{\alpha}$  of all four plasticized PLA formulations with cinnamates, is below 50 °C, this change from a rigid to a rubbery-like state can be seen by the storage moduli at 50 °C. While neat PLA shows an  $E'$  value of 1598.3 MPa, (close to the value measured at room temperature), the  $E'$  values for all cinnamate-plasticized PLA formulations are noticeably lower (<5 MPa). The plasticization effect can also be observed by the  $\tan \delta$  peak shape since plasticized formulations offer a broader peak. This effect can be estimated by measuring the full-width at half-maximum (FWHM) as seen in Table 6. A plasticized formulation usually leads to micro heterogeneities in composition inside the amorphous regions, in which the plasticizer enters preferentially. This leads to a differential interaction between PLA chains and PLA-plasticizer molecules, which in turn, provides a broader temperature range for the glass transition, resulting in higher FWHM values.<sup>[31]</sup> This broadening effect of plasticizers on the  $\tan \delta$  peak was also observed by Ivorra-Martinez et al.<sup>[64]</sup> in plasticized PLA with dibutyl itaconate (DBI). They observed a decrease in  $T_{\alpha}$  from 68.7 (neat PLA) to 39.7 °C for the plasticized formulation containing 20 wt% DBI. The corresponding elongation at break for this plasticizer content was 262%, thus showing the high efficiency of the proposed cinnamic acid esters as green plasticizers for PLA.

#### 4. Conclusions

The present work has addressed the potential of several cinnamic acid esters as green plasticizers for PLA with improved ductile properties. MC, IBC, and AC have revealed exceptional plasticization efficiency, with a noticeable increase in elongation at break of neat PLA (3.9%), up to 285%, 250%, and 339.4%, respectively, when incorporated at a constant proportion of 20 wt%. In parallel to this improvement in ductility, the impact strength is also improved, thus showing the potential of these plasticizers to improve toughness. This exceptional plasticization is directly related to a decrease in the glass transition temperature ( $T_g$ ) due to increased polymer chain-to-polymer chain interactions and increased chain mobility. The  $T_g$  of neat PLA, located at 61.7 °C (as obtained by DSC), was reduced down to values of 36.1 °C for the plasticized PLA formulation containing AC, and a remarkable in-

crease in the maximum degree of crystallinity from 18.8% (neat PLA) up to 44.4% for allyl cinnamate-plasticized PLA. Despite all cinnamates used in this study showing a boiling point above 250 °C, and the typical processing temperature of PLA by injection molding is 180–190 °C, some plasticizer is removed during processing. The extent of the lost plasticizer can be assessed by TGA. Although the nominal content of the different cinnamates was 20 wt%, the actual plasticizer content was confirmed by TGA with values of 17.7, 18.6, and 14.3 wt% for methyl trans-cinnamate, IBC, and allyl cinnamate, respectively, while the remaining plasticizer in ethyl cinnamate-plasticized PLA was about 10.9 wt%, which is not enough to trigger the plasticization mechanisms on PLA. The plasticization efficiency of some cinnamates is comparable, or even superior, to that obtained with conventional plasticizers for PLA, such as triethyl citrate (TEC), ATBC, and PEG, among others, thus showing the potential of esters of cinnamic acid as green plasticizers for PLA with improved ductile properties.

#### Acknowledgements

This research is a part of the grant PID2020-116496RB-C22, funded by MCIN/AEI/10.13039/501100011033 and the grant TED2021-131762A-I00, funded by MCIN/AEI/10.13039/501100011033 and by the European Union “NextGenerationEU”/PRTR. Authors also thank Generalitat Valenciana-GVA for funding this research through the grant numbers AICO/2021/025 and CIGE/2021/094. Funding for open access charge: Universitat Politècnica de València. Funded with Aid for First Research Projects (PAID-06-22), Vice-rectorate for Research of the Universitat Politècnica de València (UPV). Jaume Gomez-Caturla wants to thank Generalitat Valenciana-GVA, for his FPI grant (ACIF/2021/185) and grant FPU20/01732 funded by MCIN/AEI/10.13039/501100011033 and by ESF Investing in your future. Juan Ivorra-Martinez wants to thank FPU19/01759 grant funded by MCIN/AEI/10.13039/501100011033 and by ESF Investing in your future. Virginia Moreno wants to thank Generalitat Valenciana-GVA for funding a postdoc position through the APOSTD program co-funded by ESF Investing in your future, grant number CIA-POS/2021/67. D. Lascano acknowledges the Margarita Salas postdoctoral grant from the Ministerio de Universidades, Spain, funded by the European Union-Next Generation EU. Microscopy Services at UPV are also acknowledged by their help in collecting and analyzing images. After initial online publication, the spelling of the name of the first author, A.B., was corrected on March 22, 2023.

Open access funding provided by Universitat Politècnica de Valencia within the CRUE/UNIRIS gold Agreement.

#### Conflict of Interest

The authors declare no conflict of interest.

#### Data Availability Statement

The data that support the findings of this study are available from the corresponding author upon reasonable request.

#### Keywords

ductility, plasticizers, polylactide, reactive extrusion, terpenoids

Received: January 20, 2023

Revised: February 23, 2023

Published online: March 16, 2023

- [1] S. A. Rafiqah, A. Khalina, A. S. Harmaen, I. A. Tawakkal, K. Zaman, M. Asim, M. N. Nurrazi, C. H. Lee, *Polymers* **2021**, *13*, 1436.
- [2] T. Debuissy, E. Pollet, L. Avérous, *Eur. Polym. J.* **2017**, *87*, 84.
- [3] K. J. Jem, B. Tan, *Adv. Ind. Eng. Polym. Res.* **2020**, *3*, 60.
- [4] C. Pavon, M. Aldas, J. López-Martínez, S. Ferrándiz, *Polymers* **2020**, *12*, 334.
- [5] A. Z. Naser, I. Deiab, B. M. Darras, *RSC Adv.* **2021**, *11*, 17151.
- [6] Q. Zhang, M. Song, Y. Xu, W. Wang, Z. Wang, L. Zhang, *Prog. Polym. Sci.* **2021**, *120*, 101430.
- [7] C. Vilela, A. F. Sousa, A. C. Fonseca, A. C. Serra, J. F. J. Coelho, C. S. R. Freire, A. J. D. Silvestre, *Polym. Chem.* **2014**, *5*, 3119.
- [8] M. S. Singhvi, S. S. Zinjarde, D. V. Gokhale, *J. Appl. Microbiol.* **2019**, *127*, 1612.
- [9] A. N. Vaidya, R. A. Pandey, S. Mudliar, M. S. Kumar, T. Chakrabarti, S. Devotta, *Crit. Rev. Environ. Sci. Technol.* **2005**, *35*, 429.
- [10] K. Fukushima, K. Sogo, S. Miura, Y. Kimura, *Macromol. Biosci.* **2004**, *4*, 1021.
- [11] C. Pavon, M. Aldas, M. D. Samper, D. L. Motoc, S. Ferrándiz, J. López-Martínez, *Polymers* **2022**, *14*, 2646.
- [12] K. M. Nampoothiri, N. R. Nair, R. P. John, *Bioresour. Technol.* **2010**, *101*, 8493.
- [13] S. Xu, J.-F. Tahon, I. De-Waele, G. Stoclet, V. Gaucher, *eXPRESS Polym. Lett.* **2020**, *14*, 1034.
- [14] L. Quiles-Carrillo, S. Duarte, N. Montanes, S. Torres-Giner, R. Balart, *Mater. Des.* **2018**, *140*, 54.
- [15] L. Quiles-Carrillo, M. M. Blanes-Martínez, N. Montanes, O. Fenollar, S. Torres-Giner, R. Balart, *Eur. Polym. J.* **2018**, *98*, 402.
- [16] P. Xiang, S. Bi, F. Mei, C. Deng, D. Yu, X. Chen, P. Yu, *Macromol. Mater. Eng.* **2021**, *306*, 2100426.
- [17] R. Salehiyan, S. S. Ray, V. Ojijo, *Macromol. Mater. Eng.* **2018**, *303*, 1800349.
- [18] K. Kultravut, K. Kuboyama, T. Ougizawa, *Macromol. Mater. Eng.* **2019**, *304*, 1900323.
- [19] S. Su, R. Kopitzky, S. Tolga, S. Kabasci, *Polymers* **2019**, *11*, 1193.
- [20] M. J. Garcia-Campo, L. Quiles-Carrillo, L. Sanchez-Nacher, R. Balart, N. Montanes, *Polym. Bull.* **2019**, *76*, 1839.
- [21] H. Cai, C. Cao, Y. Zheng, D. Liu, X. Xia, X. Sun, X. Liu, L. Xiao, Q. Qian, Q. Chen, *Macromol. Mater. Eng.* **2022**, 2200581.
- [22] J. M. Ferri, O. Fenollar, A. Jorda-Vilaplana, D. García-Sanoguera, R. Balart, *Polym. Int.* **2016**, *65*, 453.
- [23] L. Aliotta, A. Vannozzi, I. Canesi, P. Cinelli, M. B. Coltelli, A. Lazzeri, *Polymers* **2021**, *13*, 218.
- [24] W. Chen, C. Qi, Y. Li, H. Tao, *Radiat. Phys. Chem.* **2021**, *180*, 109239.
- [25] M. Nofar, R. Salehiyan, U. Ciftci, A. Jalali, A. Durmus, *Composites, Part B* **2020**, *182*, 107661.
- [26] A. Carbonell-Verdu, J. M. Ferri, F. Dominici, T. Boronat, L. Sanchez-Nacher, R. Balart, L. Torre, *eXPRESS Polym. Lett.* **2018**, *12*, 808.
- [27] J. M. Ferri, D. Garcia-Garcia, A. Carbonell-Verdu, O. Fenollar, R. Balart, *J. Appl. Polym. Sci.* **2018**, *135*, 45751.
- [28] M. J. Garcia-Campo, L. Quiles-Carrillo, J. Masia, M. J. Reig-Perez, N. Montanes, R. Balart, *Materials* **2017**, *10*, 1339.
- [29] J. Gonzalez-Ausejo, E. Sanchez-Safont, J. M. Lagaron, R. Balart, L. Cabedo, J. Gamez-Perez, *J. Appl. Polym. Sci.* **2017**, *134*, 44806.
- [30] M. Rahman, C. Brazel, *Prog. Polym. Sci.* **2004**, *29*, 1223.
- [31] M. Maiza, M. T. Benaniba, V. Massardier-Nageotte, *J. Polym. Eng.* **2016**, *36*, 371.
- [32] M. Bocqué, C. Voirin, V. Lapinte, S. Caillol, J.-J. Robin, *J. Polym. Sci., Part A: Polym. Chem.* **2016**, *54*, 11.
- [33] B. Brüster, C. Amozoqueño, P. Gryan, I. Peral, B. Watts, J. M. Raquez, P. Dubois, F. Addiego, *Macromol. Mater. Eng.* **2017**, *302*, 1700326.
- [34] T. Tabi, T. Ageyeva, J. G. Kovacs, *Polym. Test.* **2021**, *101*, 107282.
- [35] M. A. Shirai, M. V. E. Grossmann, S. Mali, F. Yamashita, P. S. Garcia, C. M. O. Müller, *Carbohydr. Polym.* **2013**, *92*, 19.
- [36] K. Zawada, A. Plichta, D. Janczewski, H. Hajmowicz, Z. Florjanczyk, M. Stepien, A. Sobiecka, L. Synoradzki, *ACS Sustainable Chem. Eng.* **2017**, *5*, 5999.
- [37] M. A. Shirai, C. M. O. Müller, M. V. E. Grossmann, F. Yamashita, *J. Polym. Environ.* **2015**, *23*, 54.
- [38] K. Gzyra-Jagiela, K. Sulak, Z. Draczynski, S. Podzimek, S. Galecki, S. Jagodzinska, D. Borkowski, *Polymers* **2021**, *13*, 3651.
- [39] T. Mekonnen, P. Mussone, H. Khalil, D. Bressler, *J. Mater. Chem. A* **2013**, *1*, 13379.
- [40] N. Petchwattana, J. Sanetuntikul, B. Narupai, *J. Polym. Environ.* **2018**, *26*, 1160.
- [41] A. Carbonell-Verdu, D. Garcia-Garcia, F. Dominici, L. Torre, L. Sanchez-Nacher, R. Balart, *Eur. Polym. J.* **2017**, *91*, 248.
- [42] J. M. Ferri, D. Garcia-Garcia, N. Montanes, O. Fenollar, R. Balart, *Polym. Int.* **2017**, *66*, 882.
- [43] A. Carbonell-Verdu, M. D. Samper, D. Garcia-Garcia, L. Sanchez-Nacher, R. Balart, *Ind. Crops Prod.* **2017**, *104*, 278.
- [44] J. M. Ferri, M. D. Samper, D. García-Sanoguera, M. J. Reig, O. Fenollar, R. Balart, *J. Mater. Sci.* **2016**, *51*, 5356.
- [45] S. Rojas-Lema, L. Quiles-Carrillo, D. Garcia-Garcia, B. Melendez-Rodriguez, R. Balart, S. Torres-Giner, *Molecules* **2020**, *25*, 1976.
- [46] D. Li, Y. Jiang, S. Lv, X. Liu, J. Gu, Q. Chen, Y. Zhang, *PLoS One* **2018**, *13*, e0193520.
- [47] E. de Jong, A. Higson, P. Walsh, M. Wellisch, *Biofuels, Bioprod. Biorefin.* **2012**, *6*, 606.
- [48] M. Dusselier, P. Van Wouwe, A. Dewaele, E. Makshina, B. F. Sels, *Energy Environ. Sci.* **2013**, *6*, 1415.
- [49] M. Arrieta, M. Samper, M. Aldas, J. López, *Materials* **2017**, *10*, 1008.
- [50] D. W. Van Krevelen, K. T. Nijenhuis, *Properties of Polymers: Their Correlation with Chemical Structure; Their Numerical Estimation and Prediction from Additive Group Contributions*, Elsevier, Amsterdam **2009**.
- [51] C. M. Hansen, *Ind. Eng. Chem. Prod. Res. Dev.* **1969**, *8*, 2.
- [52] E. Bagley, T. Nelson, J. Scigliano, *J. Paint Technol.* **1971**, *43*, 35.
- [53] R. Auras, B. Harte, S. Selke, *Macromol. Biosci.* **2004**, *4*, 835.
- [54] L. Aliotta, I. Canesi, A. Lazzeri, *Polym. Test.* **2021**, *98*, 107163.
- [55] L. Gonzalez, A. Agüero, L. Quiles-Carrillo, D. Lascano, N. Montanes, *Materials* **2019**, *12*, 1627.
- [56] K. Adamska, A. Voelkel, A. Berlinska, *J. Pharm. Biomed. Anal.* **2016**, *127*, 202.
- [57] S. Su, *Polymers* **2021**, *13*, 2339.
- [58] L. Virág, R. Bocsi, D. Petho, *Crystals* **2022**, *12*, 1525.
- [59] L. C. Llanes, S. H. Clasen, A. T. N. Pires, I. P. Gross, *Eur. Polym. J.* **2021**, *142*, 110112.
- [60] Á. Agüero, D. Lascano, D. Garcia-Sanoguera, O. Fenollar, S. Torres-Giner, *Sustainability* **2020**, *12*, 652.
- [61] M. P. Arrieta, J. López, S. Ferrándiz, M. A. Peltzer, *Polym. Test.* **2013**, *32*, 760.
- [62] V. P. Martino, R. A. Ruseckaite, A. Jiménez, *J. Therm. Anal. Calorim.* **2006**, *86*, 707.
- [63] R. Tejada-Oliveros, S. Fiori, J. Gomez-Caturla, D. Lascano, N. Montanes, L. Quiles-Carrillo, D. Garcia-Sanoguera, *Polymers* **2022**, *14*, 1874.
- [64] J. Ivorra-Martinez, M. A. Peydro, J. Gomez-Caturla, T. Boronat, R. Balart, *Macromol. Mater. Eng.* **2022**, *307*, 2200360.
- [65] S. Kasmi, A. Gallos, J. Beaugrand, G. Paës, F. Allais, *Eur. Polym. J.* **2019**, *110*, 293.
- [66] C. Unterweger, O. Brüggemann, C. Fürst, *Polym. Compos.* **2014**, *35*, 227.
- [67] R. Ordoñez, L. Atarés, A. Chiralt, *Food Bioprod. Process.* **2022**, *133*, 25.
- [68] M. P. Arrieta, M. D. Samper, J. López, A. Jiménez, *J. Polym. Environ.* **2014**, *22*, 460.
- [69] M. P. Arrieta, L. Peponi, D. López, M. Fernández-García, *Ind. Crops Prod.* **2018**, *111*, 317.

- [70] M. Murariu, A. Da Silva Ferreira, M. Alexandre, P. Dubois, *Polym. Adv. Technol.* **2008**, *19*, 636.
- [71] S. Jacobsen, H.-G. Fritz, *Polym. Eng. Sci.* **1999**, *39*, 1303.
- [72] T. Kuang, J. Ju, T. Liu, A. Hejna, M. R. Saeb, S. Zhang, X. Peng, *Adv. Compos. Hybrid Mater.* **2022**, *5*, 948.
- [73] Z. Wang, T. Liu, J. Yang, F. Chen, Y. Fei, M. Zhong, T. Kuang, *ACS Appl. Polym. Mater.* **2022**, *4*, 9351.
- [74] D. Lascano, G. Moraga, J. Ivorra-Martinez, S. Rojas-Lema, S. Torres-Giner, R. Balart, T. Boronat, L. Quiles-Carrillo, *Polymers* **2019**, *11*, 2099.
- [75] D. Garcia-Garcia, A. Carbonell-Verdu, M. P. Arrieta, J. López-Martínez, M. D. Samper, *Polym. Degrad. Stab.* **2020**, *179*, 109259.
- [76] N. Burgos, D. Tolaguera, S. Fiori, A. Jiménez, *J. Polym. Environ.* **2014**, *22*, 227.
- [77] A. Chaos, A. Sangroniz, A. Gonzalez, M. Iriarte, J.-R. Sarasua, J. Del Río, A. Etxeberria, *Polym. Int.* **2019**, *68*, 125.
- [78] T. Tábi, T. Ageyeva, J. G. Kovács, *Mater. Today Commun.* **2022**, *32*, 103936.
- [79] M. Baiardo, G. Frisoni, M. Scandola, M. Rimelen, D. Lips, K. Ruffieux, E. Wintermantel, *J. Appl. Polym. Sci.* **2003**, *90*, 1731.
- [80] K. Shi, G. Liu, H. Sun, B. Yang, Y. Weng, *Polymers* **2022**, *14*, 4305.
- [81] H. Xiao, W. Lu, J.-T. Yeh, *J. Appl. Polym. Sci.* **2009**, *113*, 112.
- [82] I. Harte, C. Birkinshaw, E. Jones, J. Kennedy, E. DeBarra, *J. Appl. Polym. Sci.* **2013**, *127*, 1997.
- [83] A. Agüero, M. d. C. Morcillo, L. Quiles-Carrillo, R. Balart, T. Boronat, D. Lascano, S. Torres-Giner, O. Fenollar, *Polymers* **2019**, *11*, 1908.